

# A Laboratory Experiment for the Statistical Evaluation of Aerosol Retrieval (STEAR) Algorithms

G.L. Schuster<sup>1</sup>, R. Espinosa<sup>2,3</sup>, L. Ziembra<sup>1</sup>, A. Beyersdorf<sup>6</sup>, A. Rocha-Lima<sup>2,3</sup>, B. Anderson<sup>1</sup>, J. V. Martins<sup>2</sup>, O. Dubovik<sup>4,5</sup>, F. Ducos<sup>4</sup>, D. Fuertes<sup>5</sup>, T. Lapyonok<sup>4</sup>, M. Shook<sup>1</sup>, Y. Derimian<sup>4</sup>, R. Moore<sup>1</sup>

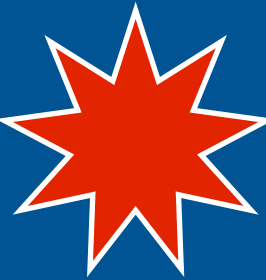
1. NASA Langley Research Center;
2. University of Maryland, Baltimore County;
3. NASA Goddard Space Flight Center;
4. Universite de Lille 1/CNRS;
5. GRASP-SAS, Remote sensing developments;
6. California State University, San Bernardino, CA.



## Acknowledgements

This material was supported by NASA through the ROSES Atmospheric Composition: Laboratory Research program, issued through the Science Mission Directorate, Earth Science Division.

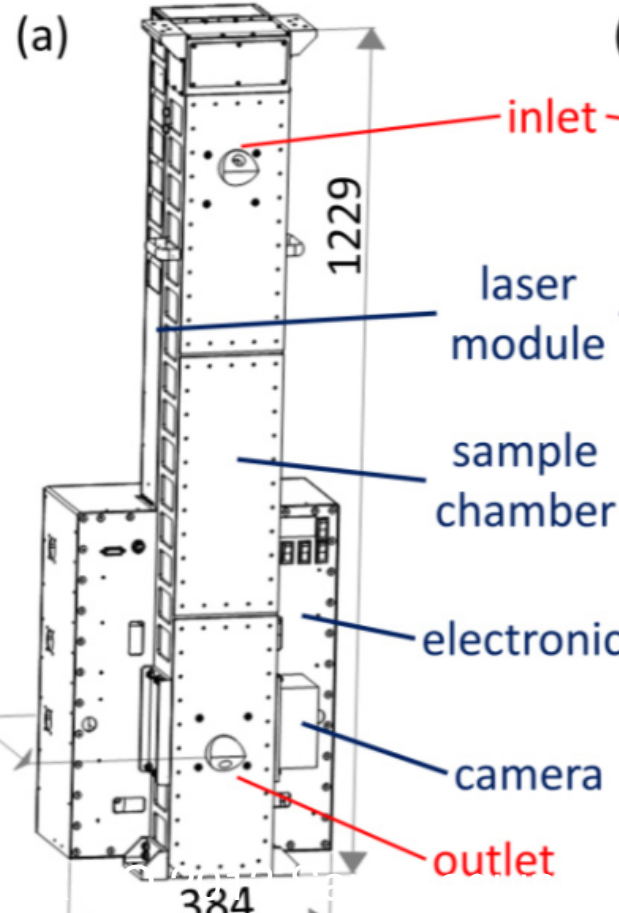
# The Difficulty of Validating AERONET Retrievals



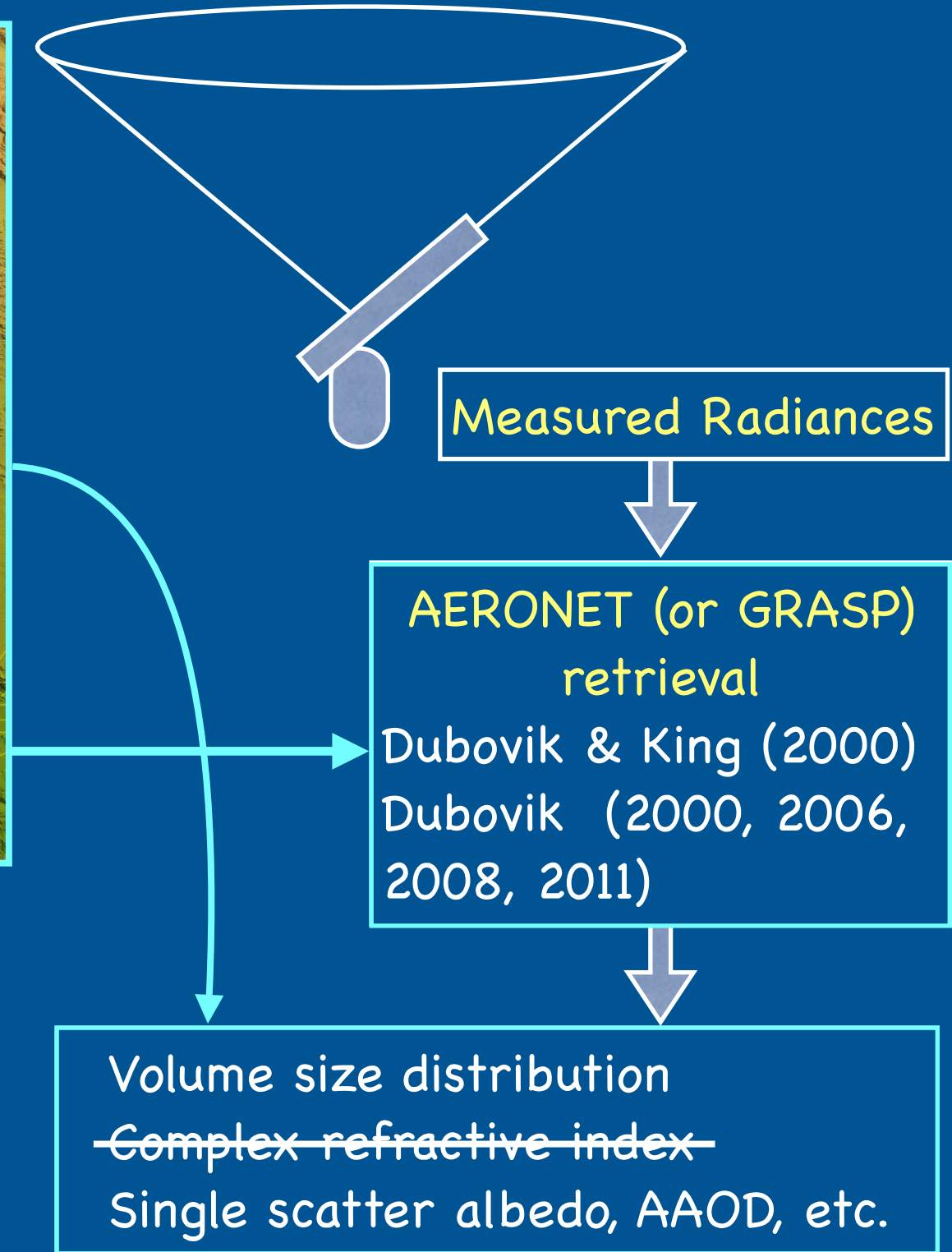
STEAR is a laboratory experiment that simulates AERONET radiances.

Fig

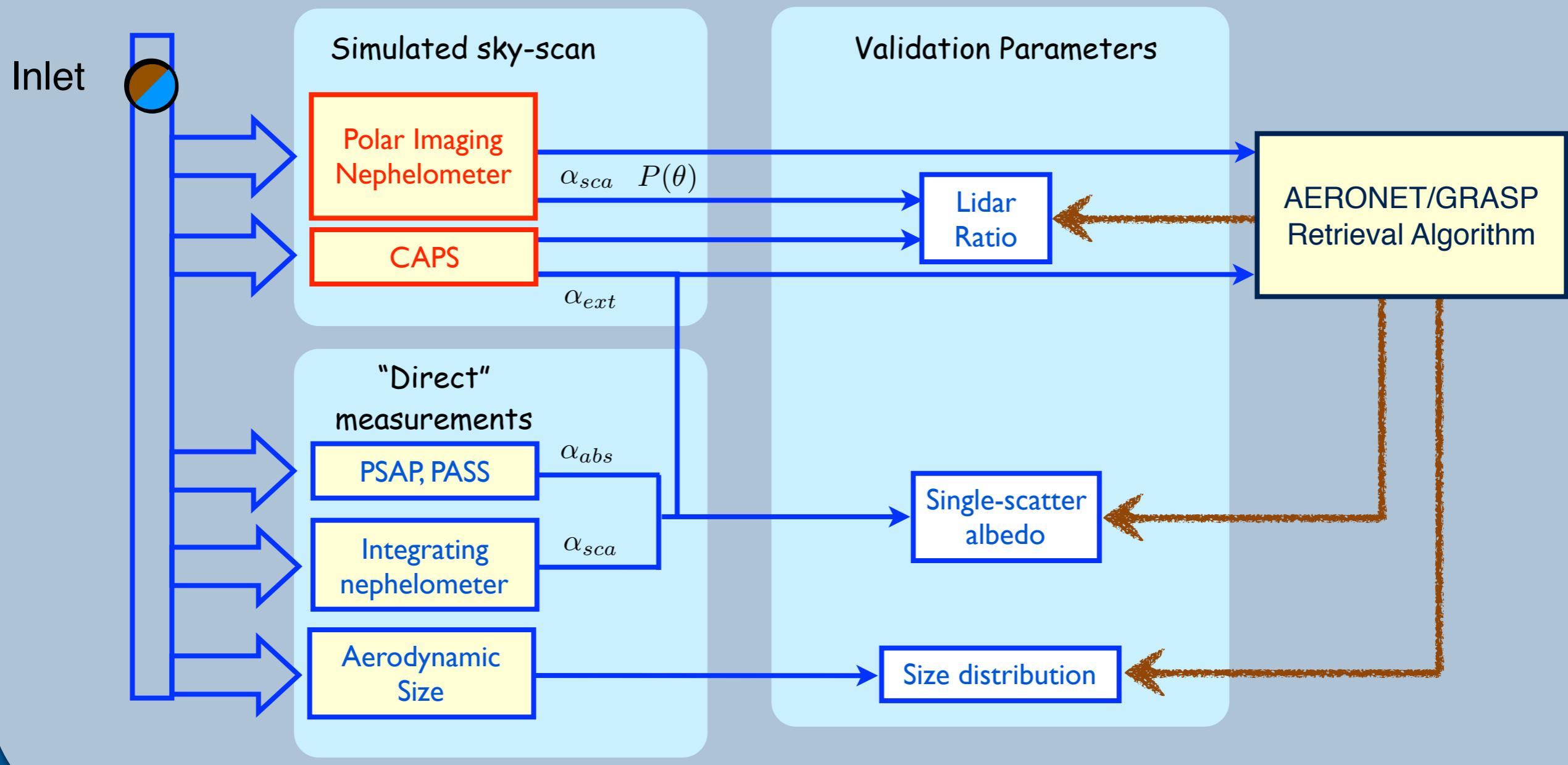
DIS  
Jim



Polarized-Imaging Nephelometer (PI-Neph)  
Dolgos and Martins (Optics Express, 2014)



# Simplified Schematic



CAPS: Cavity Attenuated Phase Shift monitor  
PSAP: Particle Soot Absorption Photometer  
PASS: Photoacoustic Soot Spectrometer

# Tested 285 samples

Tests include humidified and dried runs for both PM1 and PM2.5.

## Minerals

Hectorite  
Hematite  
Arizona Test Dust  
Cambrianshale Imt-2  
Saz-2 Ca-rich Montmorillonite  
Illite-smectite  
Na-Montmorillonite  
Montmorillonite, STx-1b  
Montmorillonite SCa-3  
Israel, Negev Desert  
Senegal  
Ripidolite CCa-2  
Palygorskite  
Arginotec NX Europe  
A1 ultrafine test dust  
Silica Dust

## Artist Pigments

Lemon Ocher  
Yellow Ocher Light  
Blue Ridge Hematite  
Brown Ocher (Goethite)  
Nicosia Yellow Ocher  
Ambrogio Yellow Earth

## Volcanic Ash

Mt. St. Helens  
Fuego Volcano  
Pinatubo  
Iceland Volcano  
Mt. St. Helens  
Puyehue  
Spurr  
Gulagong

## Soot

Ashrae #2  
120 nm soot  
105 nm Soot  
60 nm soot  
25 nm soot  
70 nm soot  
Fullerene soot

## Spheres

600 nm PSL  
900 nm PSL  
100 nm PSL

## Standards

Ammonium Sulfate  
Ammonium Nitrate  
Adipic Acid

## Mixtures

Mont STx + 5% Goethite (by mass)  
Mont STx + 10% Goethite (by mass)  
Amm Sulf + Goethite (9–26% of scat)  
Amm Sulf + Amborgio Yellow Earth (11-30% of scat)  
Amm Sulf + Italian Yellow Earth (11-38%)  
Amm Sulf + Soot (0.78–0.97 SSA)  
Internal Silica+AS  
Internal Silica+fullerene  
Internal Hematite+AS  
Internal Goethite+AS  
Internal Goethite+AS  
Internal Hematite+AS  
AS + Soot - 0.87–0.98 SSA  
AN/Full\_Int #1 + 7-15% Arginotec  
AN/Full\_Int #2 + 9-17% Mont. Sca-3  
Mont. STx, 150–1000 Mm-1  
Mont. STx, APS=0.63, 19LPM  
Mont. STx, APS=0.73, 12LPM  
Mont. STx, APS=0.94, 8LPM  
Mont. STx, APS=1.38, 5LPM  
Mont. STx, APS=1.57, 2LPM  
600 (60/Mm) + 900 nm (100/Mm) PSL  
600 (110/Mm) + 900 nm (100/Mm) PSL  
Mont. SCa-3 + Amm. Nit. (~61%)  
Mont. SCa-3 + Amm. Nit. (9–80%)  
Fullerene + Amm. Nit. (external, 0.86–0.96 SSA)  
Silica + Fullerene  
Silica + AS (Ext, 16% Dust)  
Blue Ridge Hematite + AS (Ext, 19% Dust)  
Blue Ridge Hematite + AS (Ext, 16% Dust)  
Arginotec + AS (Ext, 24% Dust)  
Arginotec + AS (Ext, 21% Dust)  
AN+Full (Ext, SSA = 0.92)  
Argintoc + AN/Full\_Ext (18% Dust, SSA = 0.92)  
Mont. Sca-3 + AN/Full\_Ext (18% Dust, SSA = 0.92)  
Mont. Sca-3 + AN/Full\_Ext (18% Dust when dry, SSA = 0.92)  
Argintoc + AN/Full\_Ext (18% Dust when dry, SSA = 0.92)

# Simulating AERONET with GRASP

- Input radiances only considered at AERONET scattering angles.
- Real refr. index range: 1.33 – 1.6
- Imag. refr. index range: 0.0005 – 0.5
- Radius range: 0.05 – 15 um (22 bins)
- Residuals less than 8%

## Some Inconsistencies

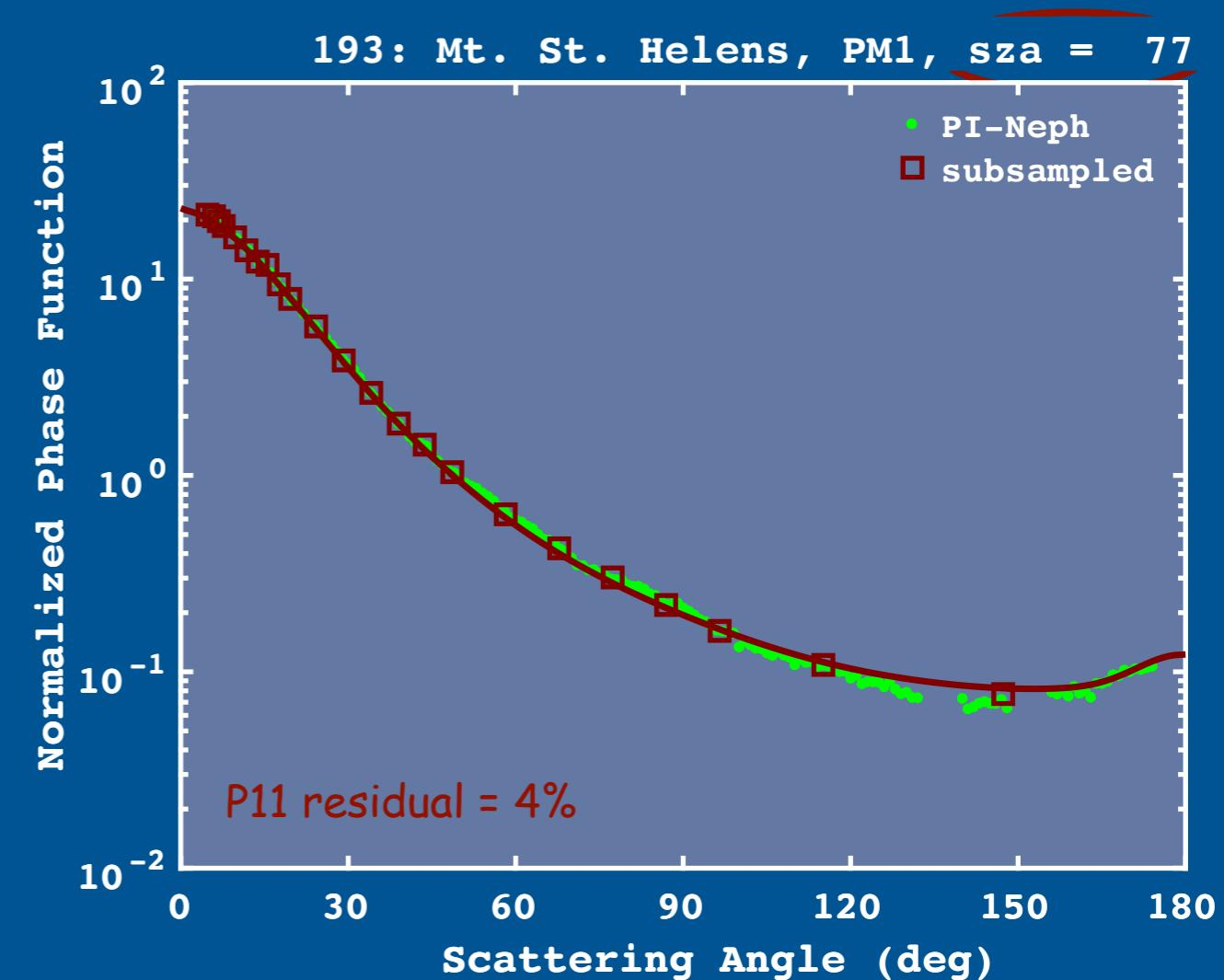
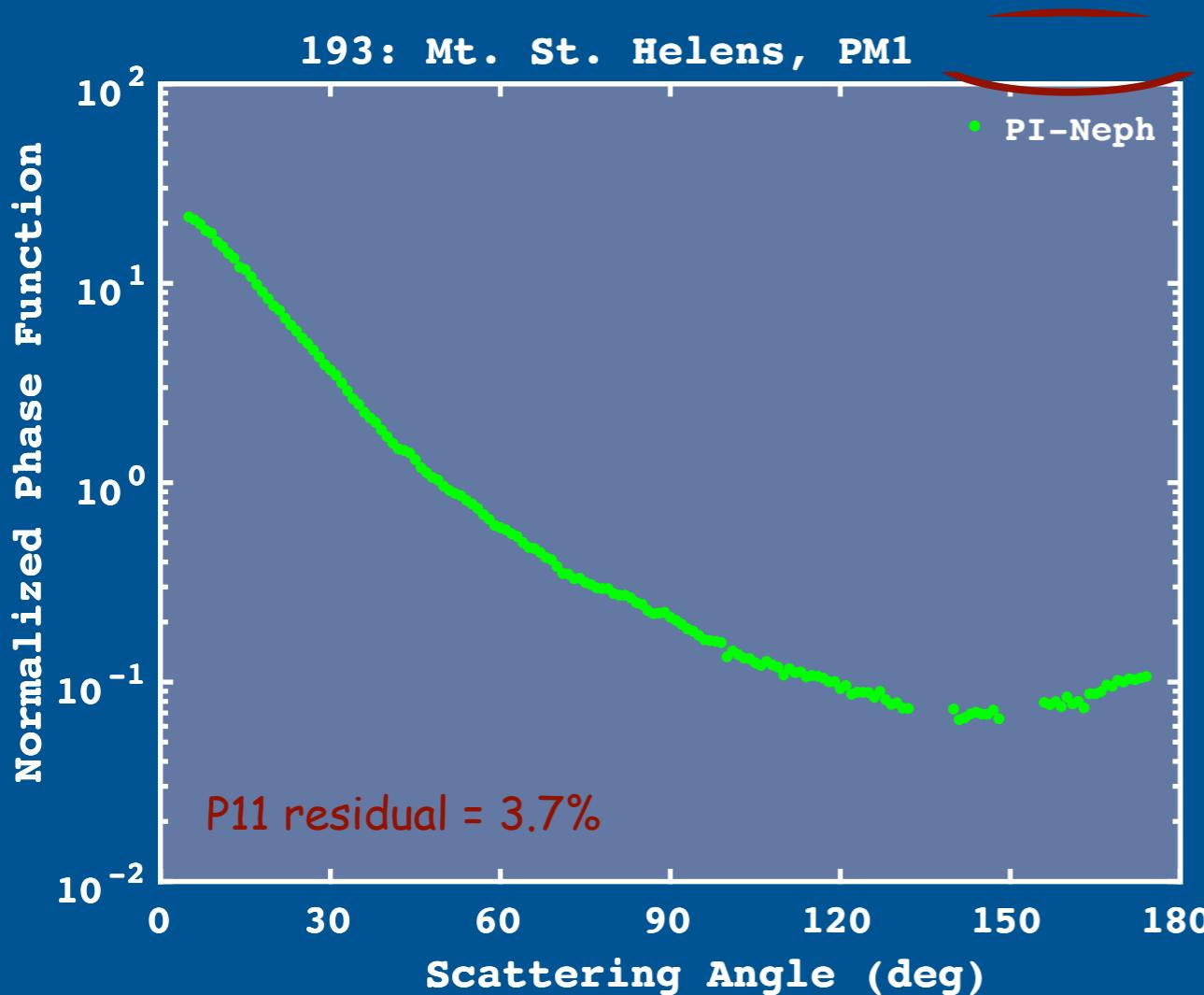
- PI-Neph wavelengths different than AERONET:
  - ▶ 473, 532, 671 nm vs 440, 675, 870, 1020 nm
- Instrument sensitivities
- No multiple scattering

“Necessary but not sufficient” experiment

# Subsampling PI-Neph to match AERONET measurement angles

- AERONET robot pauses for measurements at fixed specified azimuth angles,  $\phi$ .
- Thus, scattering angles ( $\Theta$ ) are determined by the solar zenith angle ( $\theta_o$ ) and  $\phi$ .

$$\cos \Theta = 1 - \sin^2 \theta_o (1 - \cos \phi)$$



Note: AERONET Level 2 require residuals less than 5-8%, depending upon AOD.

# Results

- Evaluate size distribution retrievals using the effective radius and effective variance
- Integrated aerosol volume
- Single-scatter albedo
- Solar zenith angle effects on the single-scatter albedo absolute bias
- Bistatic lidar ratio at 173 degrees

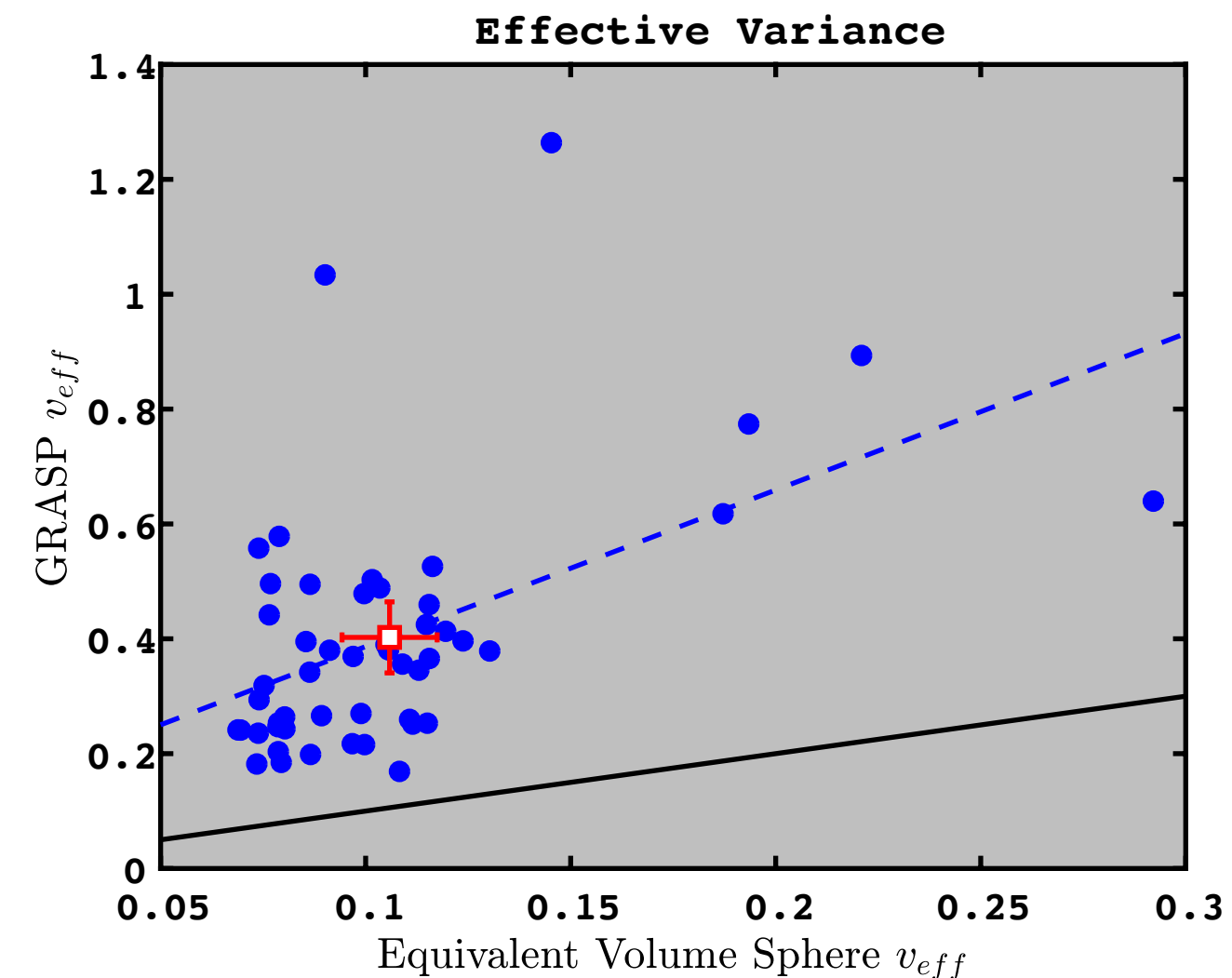
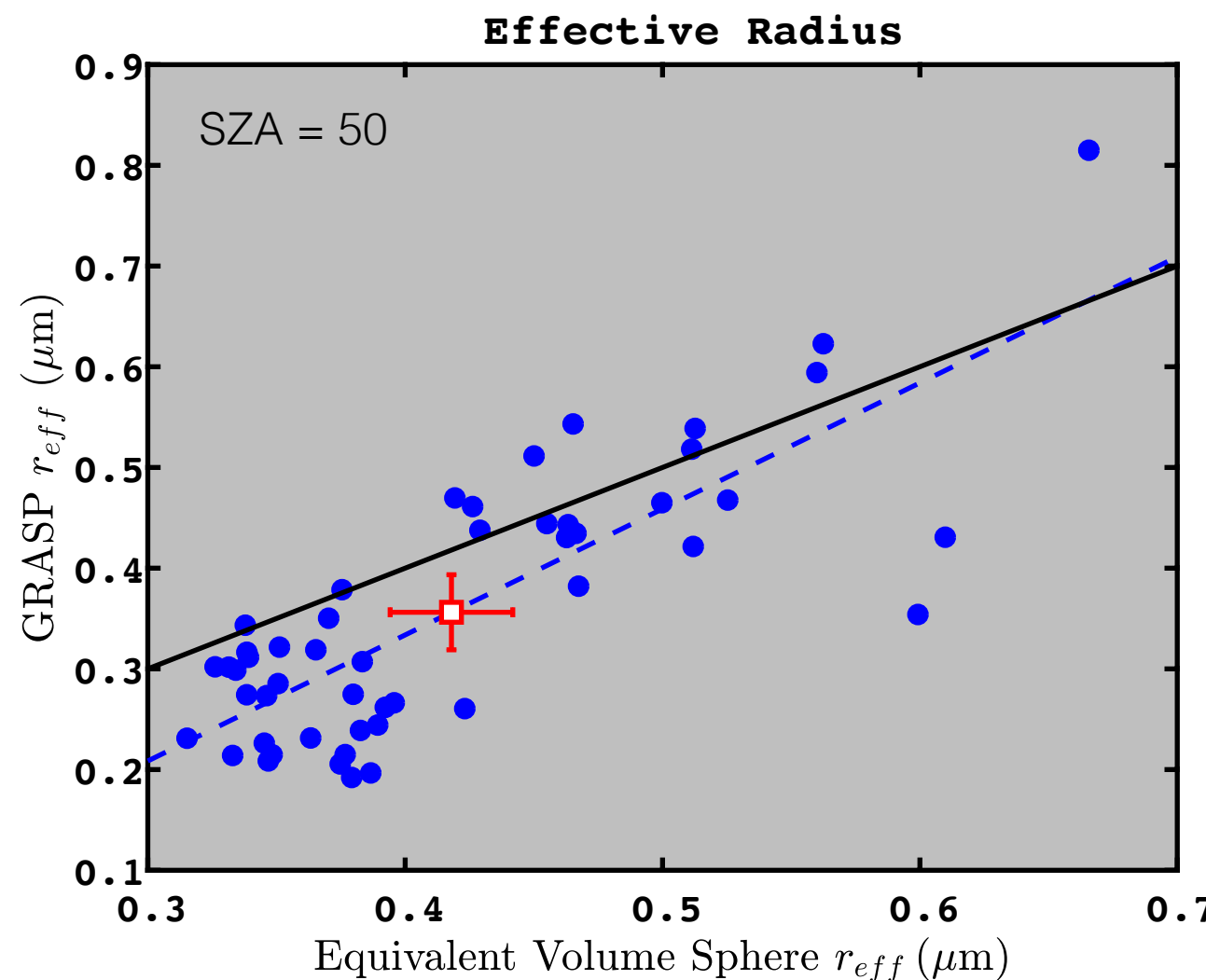
# Results

- Evaluate size distribution retrievals using the effective radius and effective variance
- Integrated aerosol volume
- Single-scatter albedo
- Solar zenith angle effects on the single-scatter albedo absolute bias
- Bistatic lidar ratio at 173 degrees

# Evaluate size distribution retrievals using the effective radius and effective variance

$$r_{eff} = \frac{\int r \times \pi r^2 n(r) dr}{\int \pi r^2 n(r) dr}$$

$$v_{eff} = \frac{\int (r - r_{eff})^2 \times \pi r^2 n(r) dr}{r_{eff}^2 \int \pi r^2 n(r) dr}$$

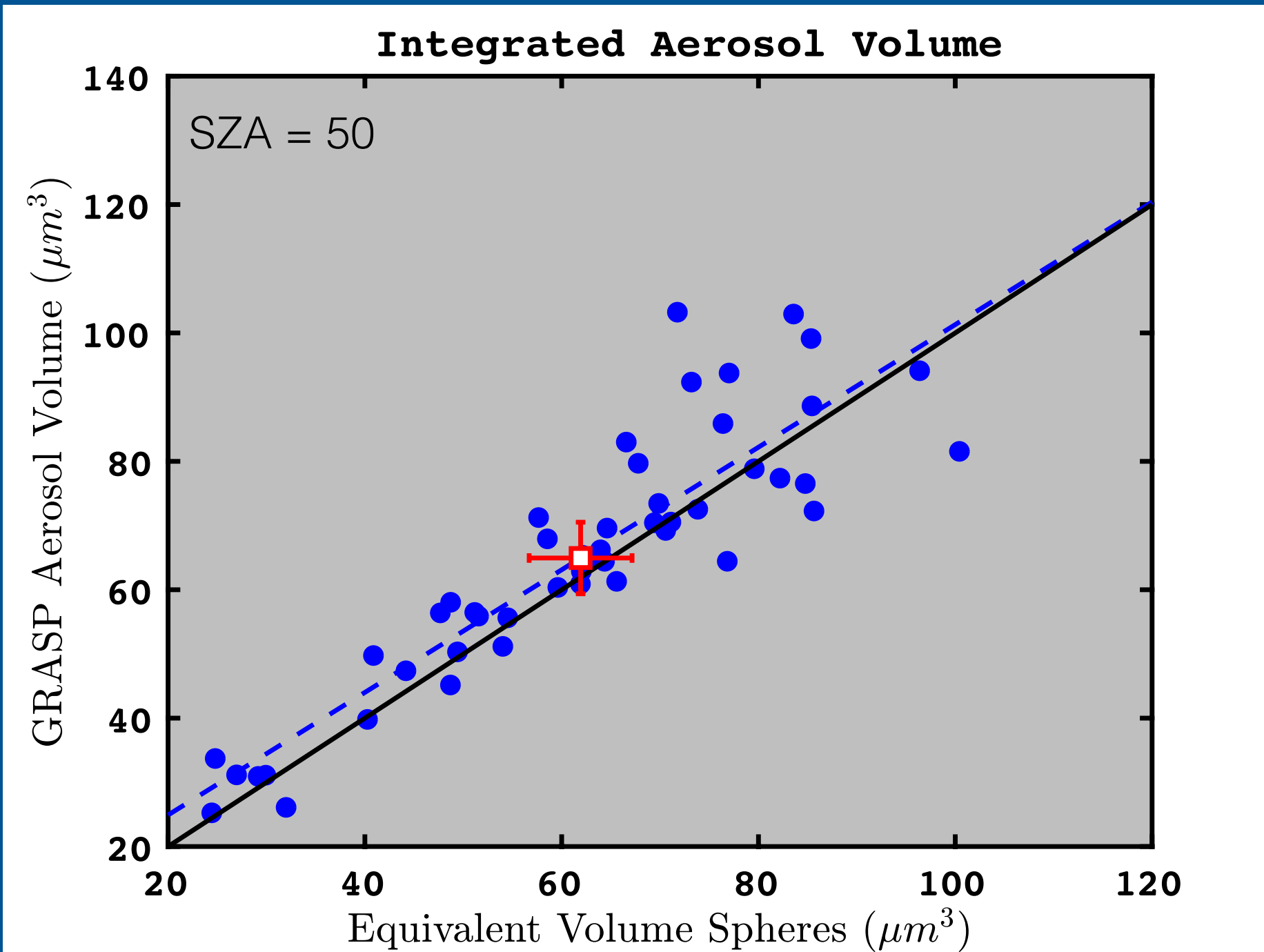


	slope	intcpt	cc	Absolute Bias	Relative Bias (%)	RMS	N	SZA	DSF
R_eff	1.284	-0.167	0.800	-0.051	-13	0.10	50	50	vrbl
V_eff	2.276	0.114	0.511	0.297	280	0.36	50	50	vrbl

# Results

- Evaluate size distribution retrievals using the effective radius and effective variance
- Integrated aerosol volume
- Single-scatter albedo
- Solar zenith angle effects on the single-scatter albedo absolute bias
- Bistatic lidar ratio at 173 degrees

# Integrated Aerosol Volume

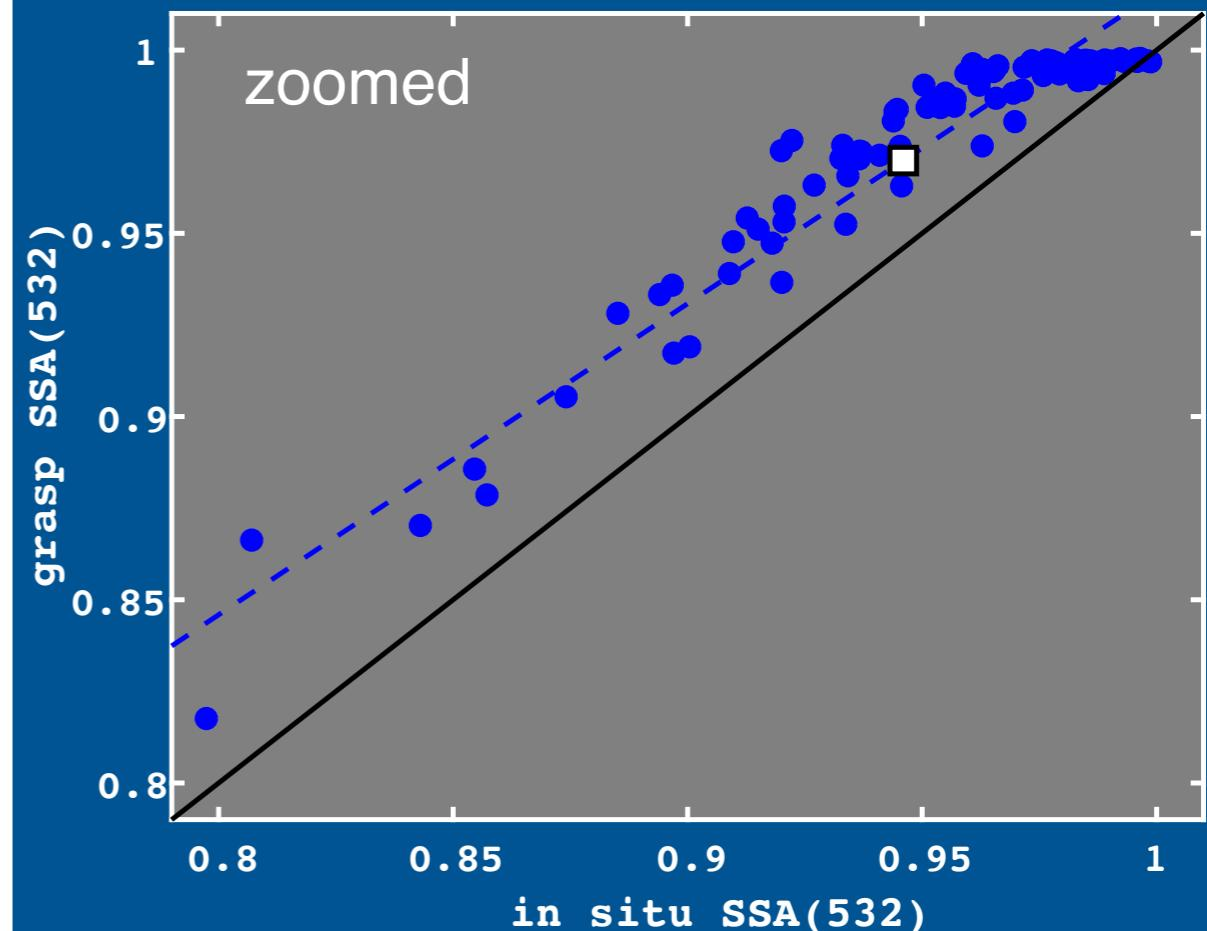
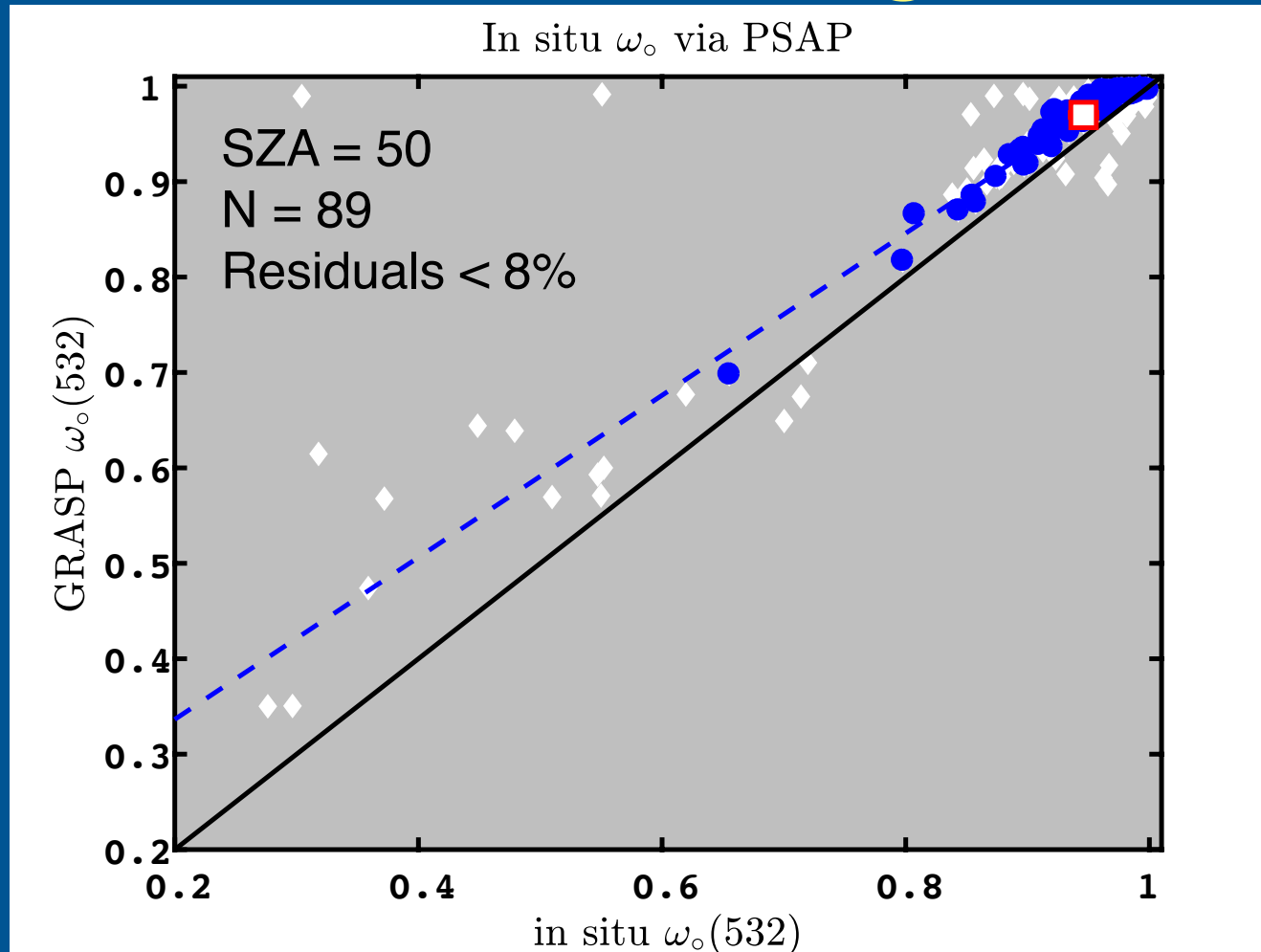


SZA	slope	intcpt	cc	Absolute Bias	Relative Bias (%)	RMS	N	DSF
50	1.031	5.812	0.896	7.604	13	11.55	50	vrbl
77	1.100	3.482	0.844	9.363	16	14.40	45	vrbl
1-deg	1.014	10.284	0.713	11.139	18	18.50	38	vrbl

# Results

- Evaluate size distribution retrievals using the effective radius and effective variance
- Integrated aerosol volume
- Single-scatter albedo
- Solar zenith angle effects on the single-scatter albedo absolute bias
- Bistatic lidar ratio at 173 degrees

# Single Scatter Albedo



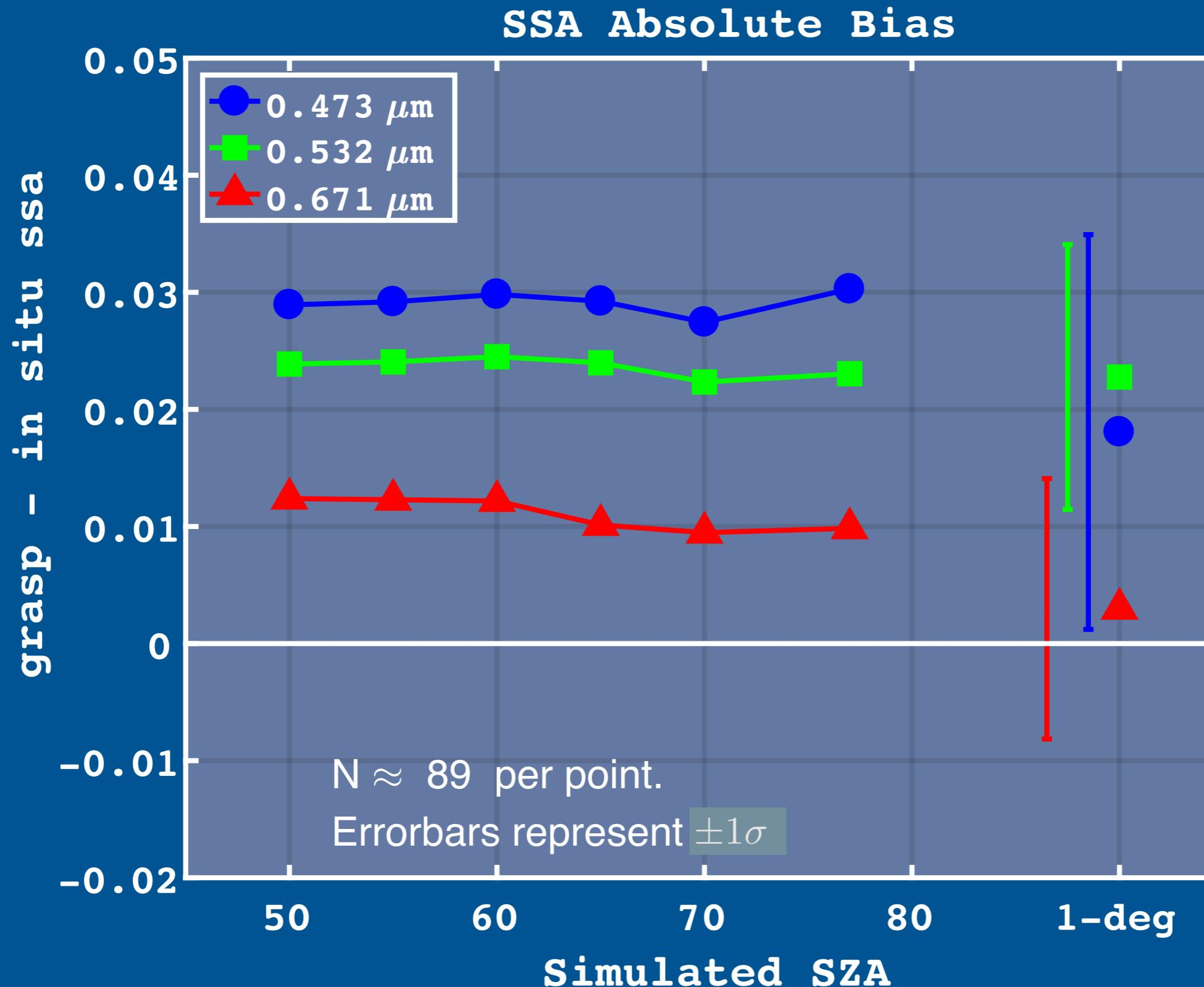
PSAP	
	$\frac{(\text{EXT} - \text{ABS}_{\text{psap}})}{\text{EXT}}$
corr. coef.	0.971
slope	0.849
intercept	0.167
abslt bias	0.024

EXT:  
Extinction via Cavity Attenuated  
Phase Shift Spectrometer  
(CAPS)

# Results

- Evaluate size distribution retrievals using the effective radius and effective variance
- Integrated aerosol volume
- Single-scatter albedo
- Solar zenith angle effects on the single-scatter albedo absolute bias
- Bistatic lidar ratio at 173 degrees

# Solar Zenith Angle effects on SSA Absolute Bias

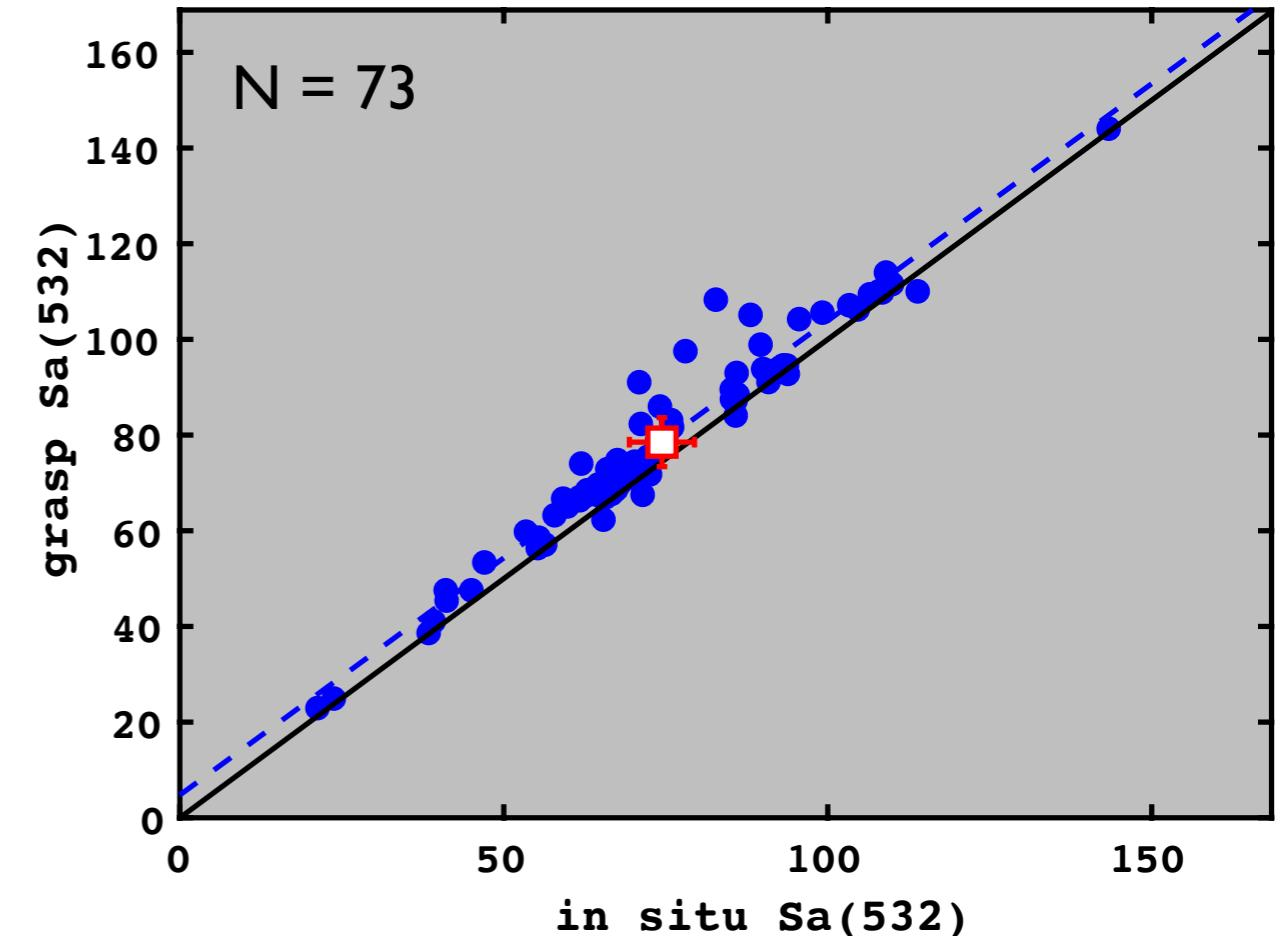
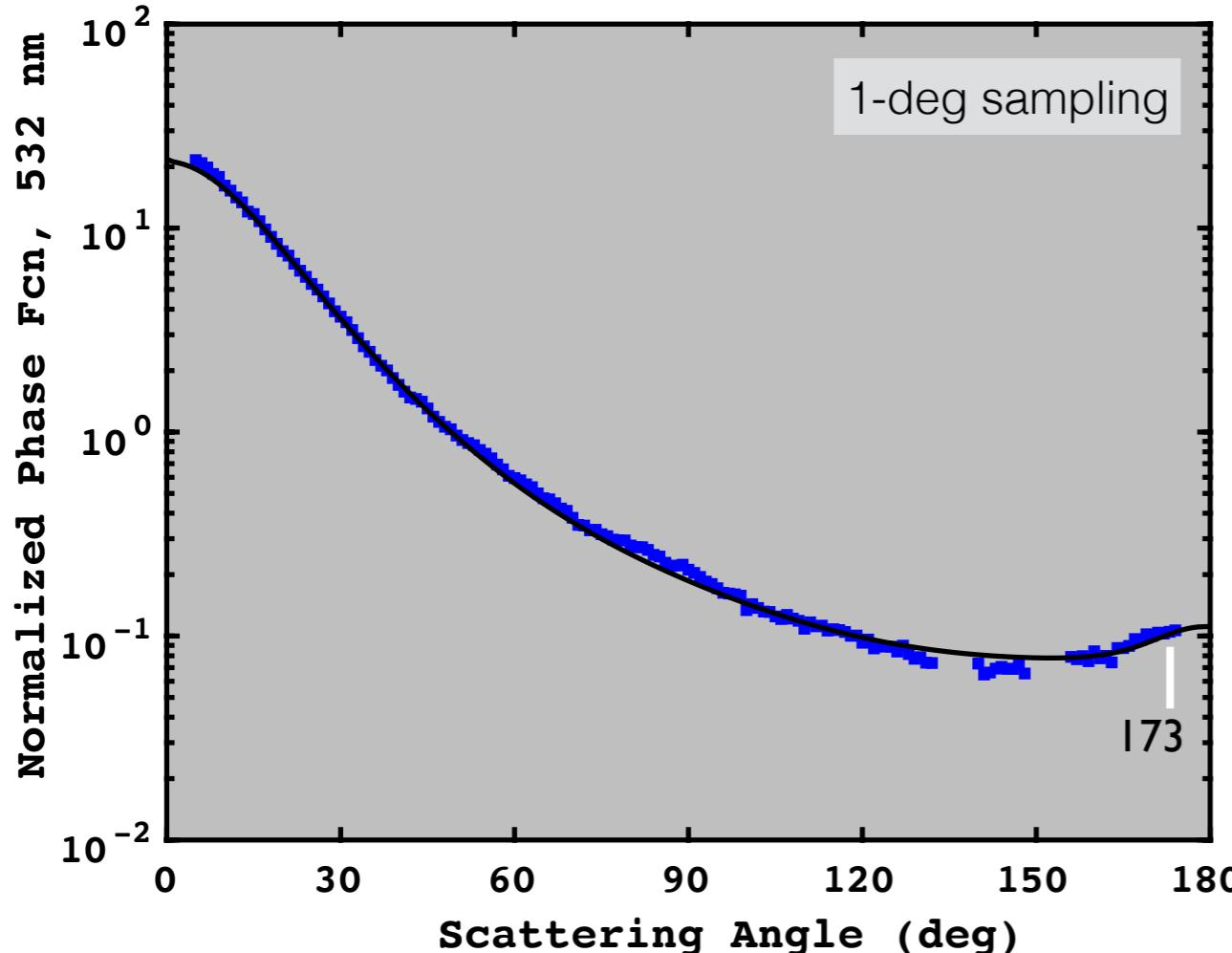


# Results

- Evaluate size distribution retrievals using the effective radius and effective variance
- Integrated aerosol volume
- Single-scatter albedo
- Solar zenith angle effects on the single-scatter albedo absolute bias
- Bistatic lidar ratio at 173 degrees

# Bistatic Lidar Ratio at 173 degrees

$$S_a = \frac{\text{ext}}{\text{sca}} \frac{4\pi}{P(173)}$$



SZA:	50	77	1-deg
correlation coef	0.714	0.860	0.973
slope:	0.774	1.004	0.991
Intercept:	19.8	7.55	4.76
Relative Bias:	2%	10%	6%
Absolute Bias:	1.8 sr	7.9 sr	4.1 sr

# Conclusions

- Simulated AERONET measurements for 285 in situ sampling volumes.
- GRASP provided quality retrievals (residuals of < 8%) for ~90 samples.
- Relative bias for effective radius is -13% when dynamic shape factor is constrained by extinction.
- Relative bias for the effective variance of size distributions is 280%.
- Relative bias for the integrated aerosol volume is 13-18% (*SZA*-dependent).
- Absolute bias for single-scatter albedo is +0.023 at 532 nm via PSAP.
- SSA biases do not vary significantly for *SZA* = 50-77 degrees.
- Relative bias for bistatic lidar ratio at 173° is 2-10%, depending upon *SZA*.

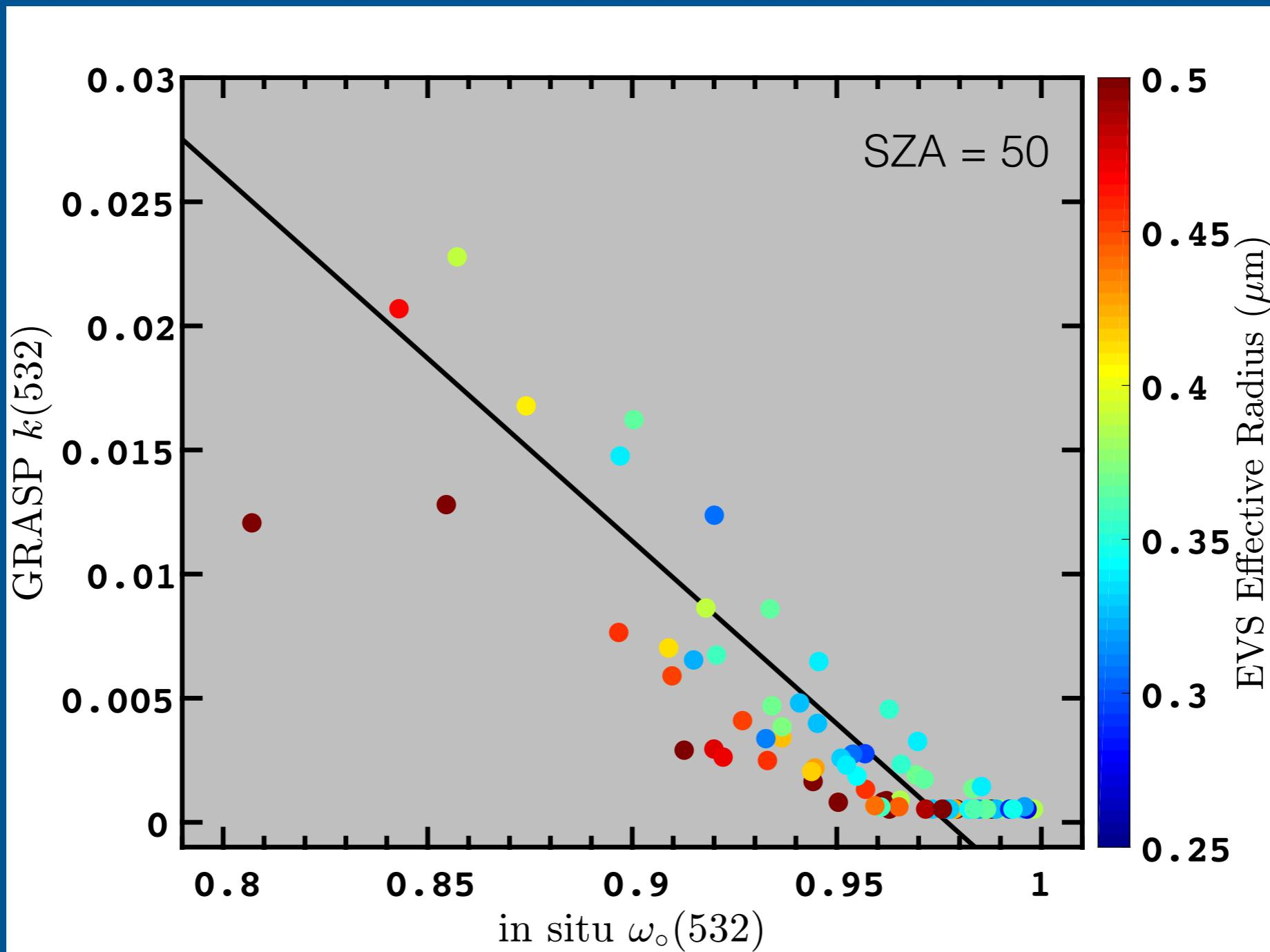
Manuscript essentially complete. To be submitted to Remote Sensing.

# Appendix

# Aerosol absorption and the single-scatter albedo

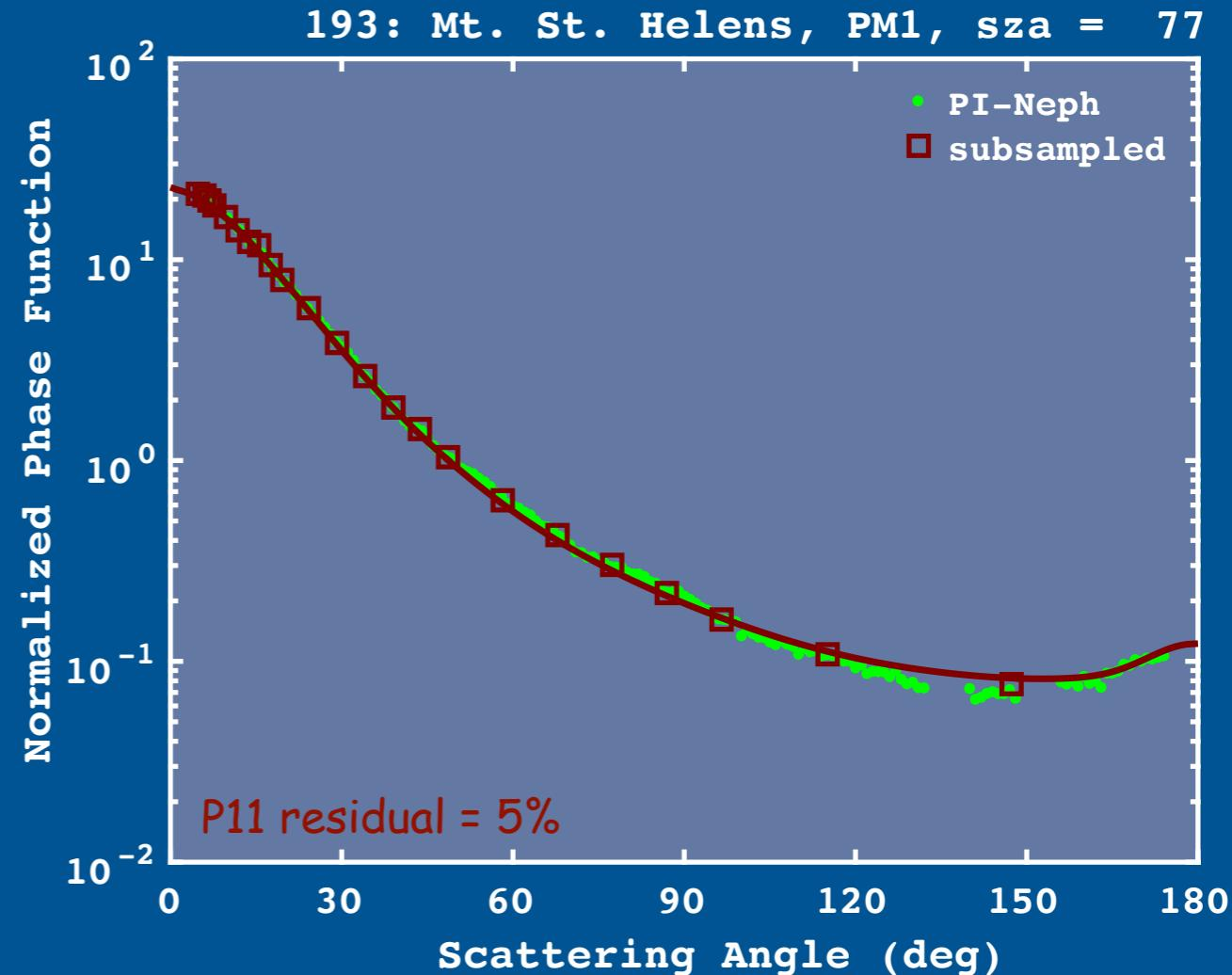
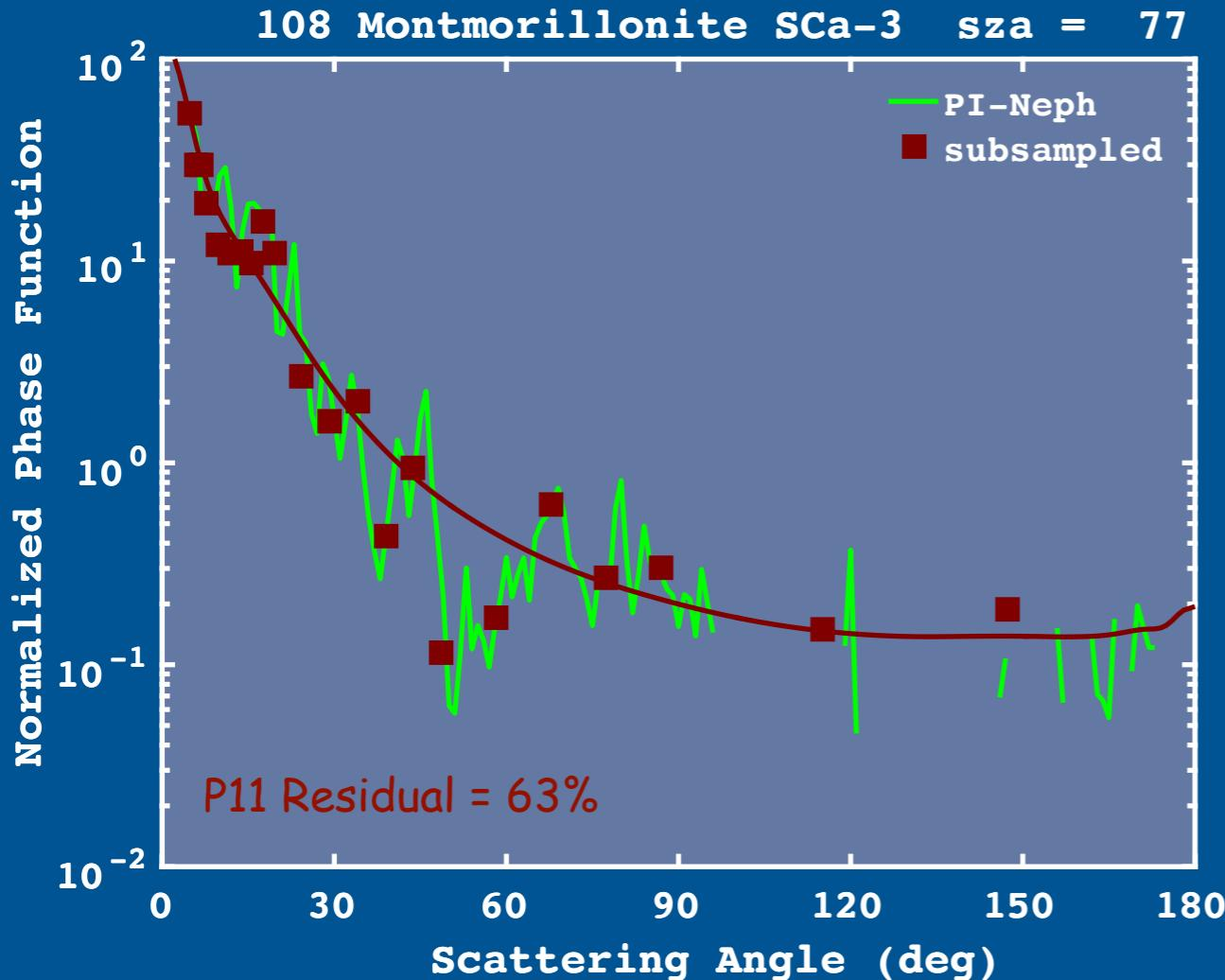
$$\alpha_{bulk}(\lambda) = \frac{4\pi k(\lambda)}{\lambda}$$

$$\omega_o = \frac{\tau_{sca}}{\tau_{ext}} = \frac{1 - \alpha}{\tau_{ext}}$$



# The Importance of Residuals

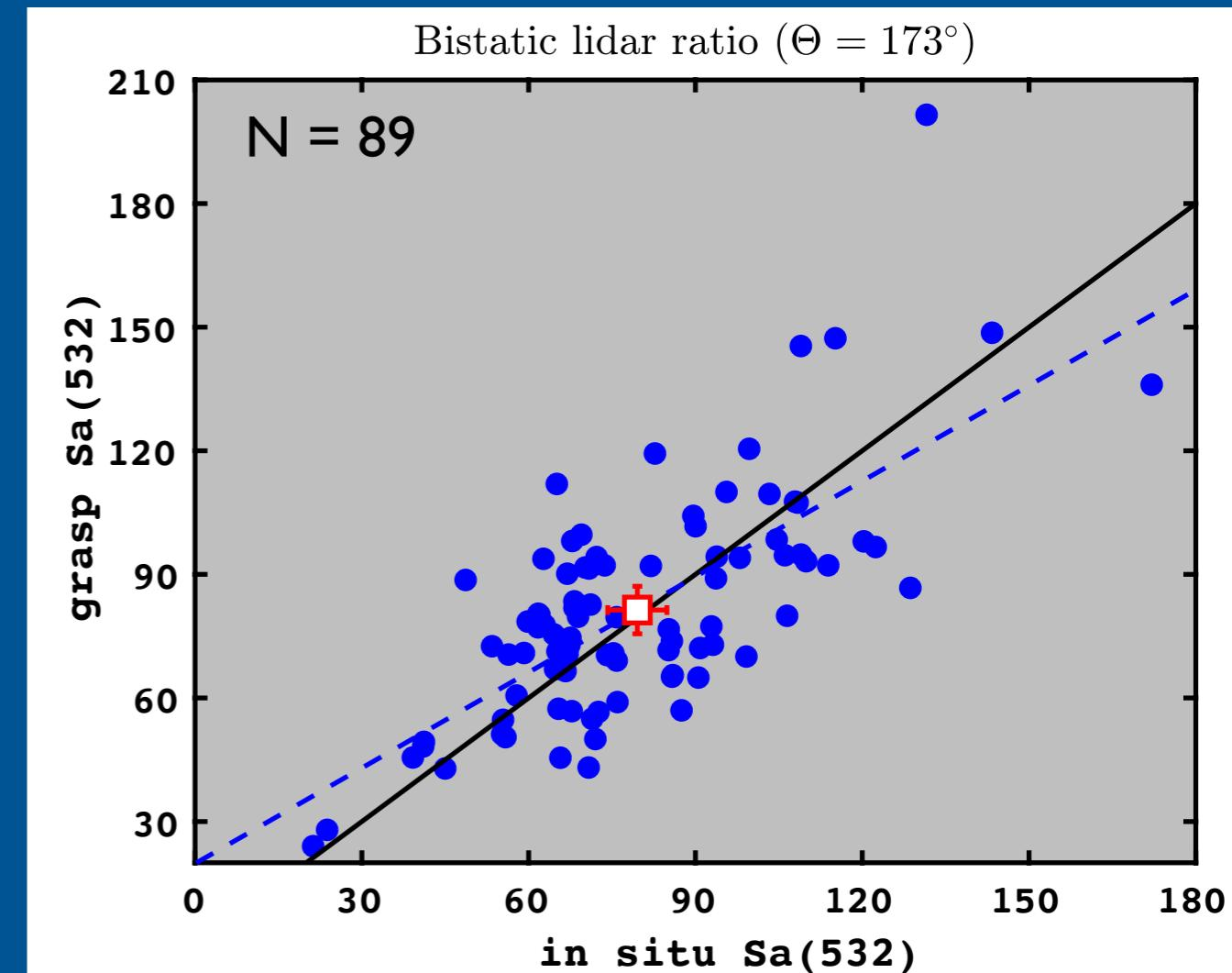
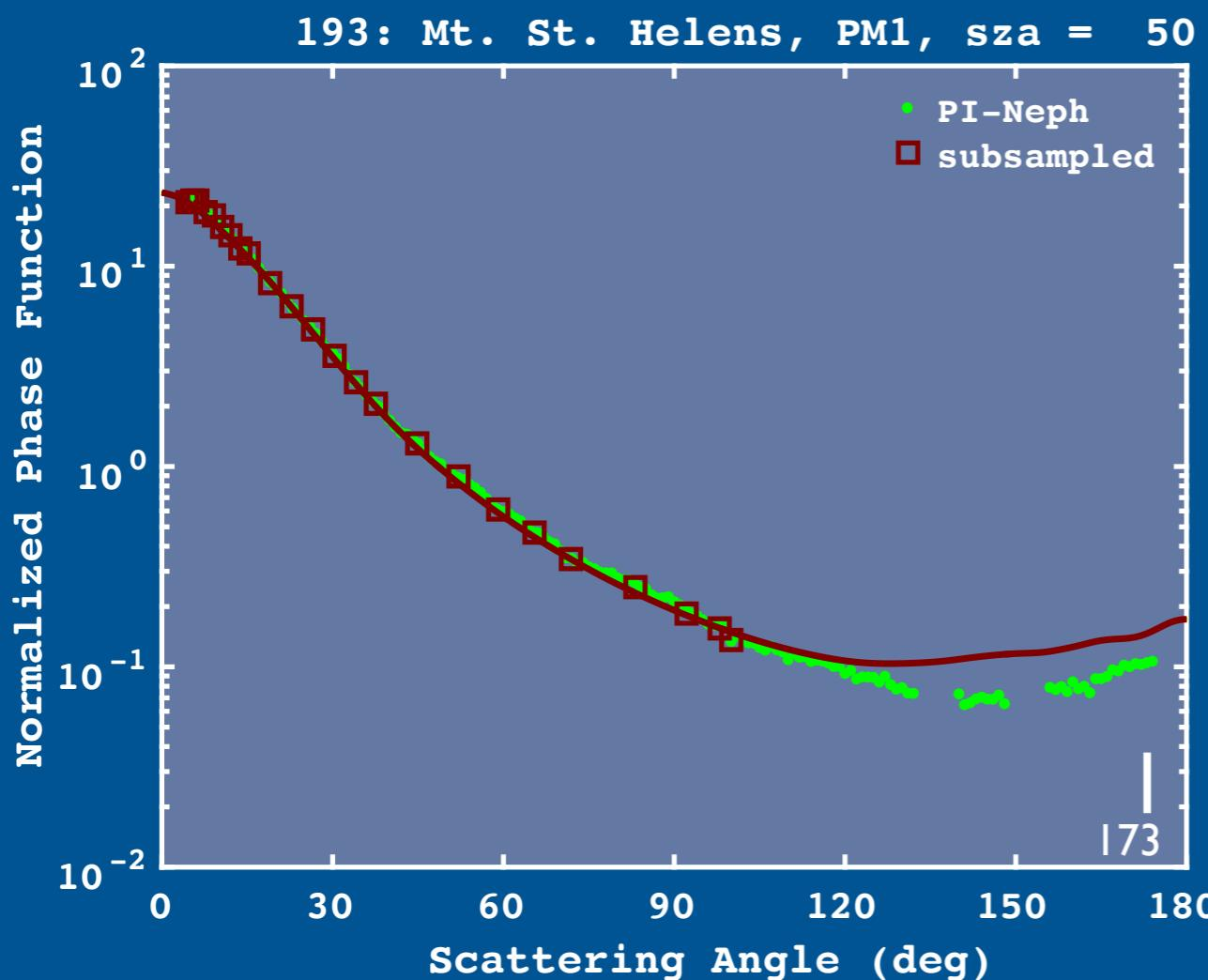
Residuals measure the ability of a retrieval model to reproduce measurements



Note: AERONET Level 2 require residuals less than 5-8%, depending upon AOD.

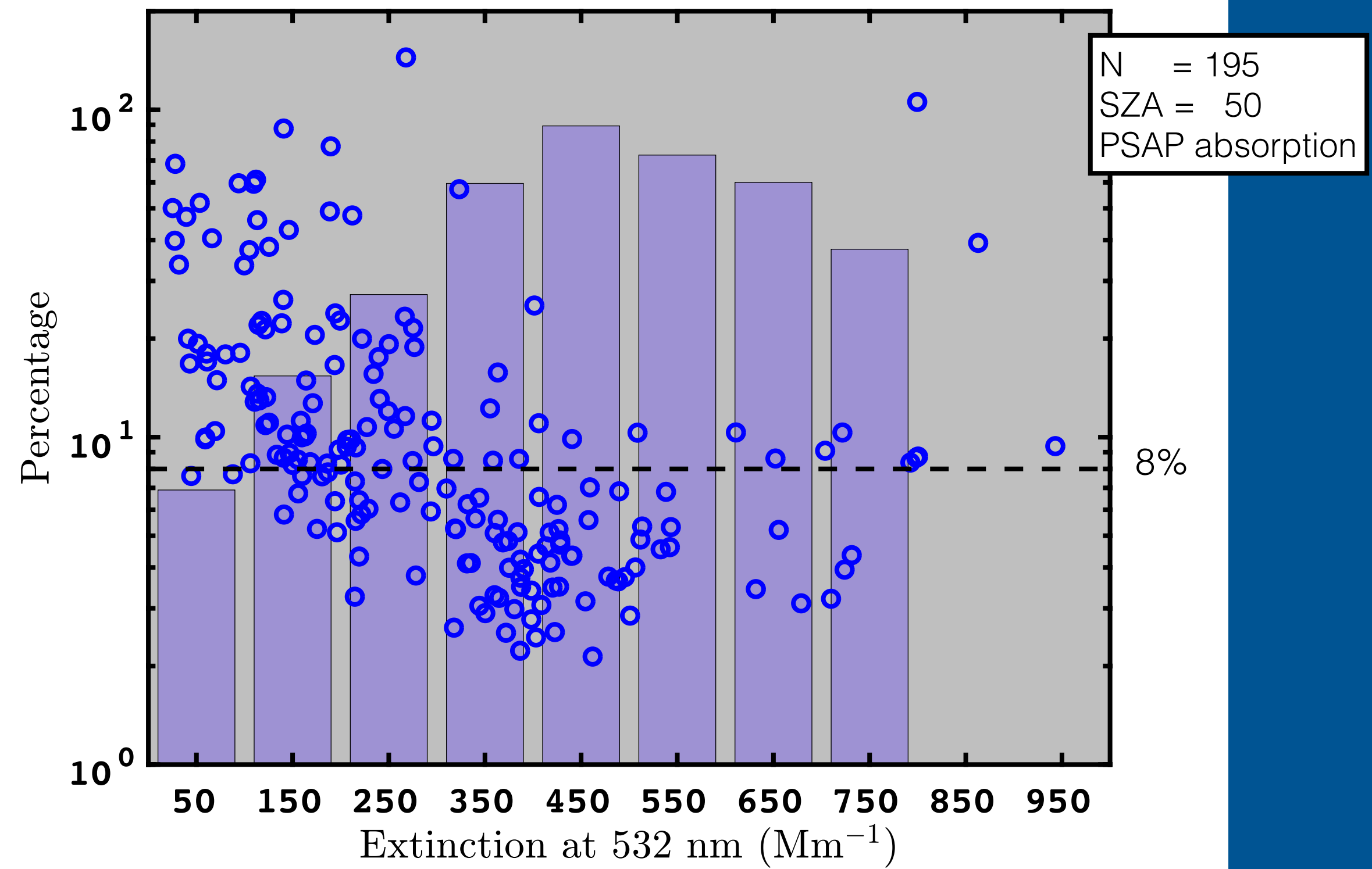
# Bistatic Lidar Ratio at 173 degrees

$$S_a = \frac{\text{ext}}{\text{sca}} \frac{4\pi}{P(173)}$$



SZA: 50	
correlation coef	0.714
slope:	0.774
Intercept:	19.8
Relative Bias:	2%
Absolute Bias:	1.79 sr

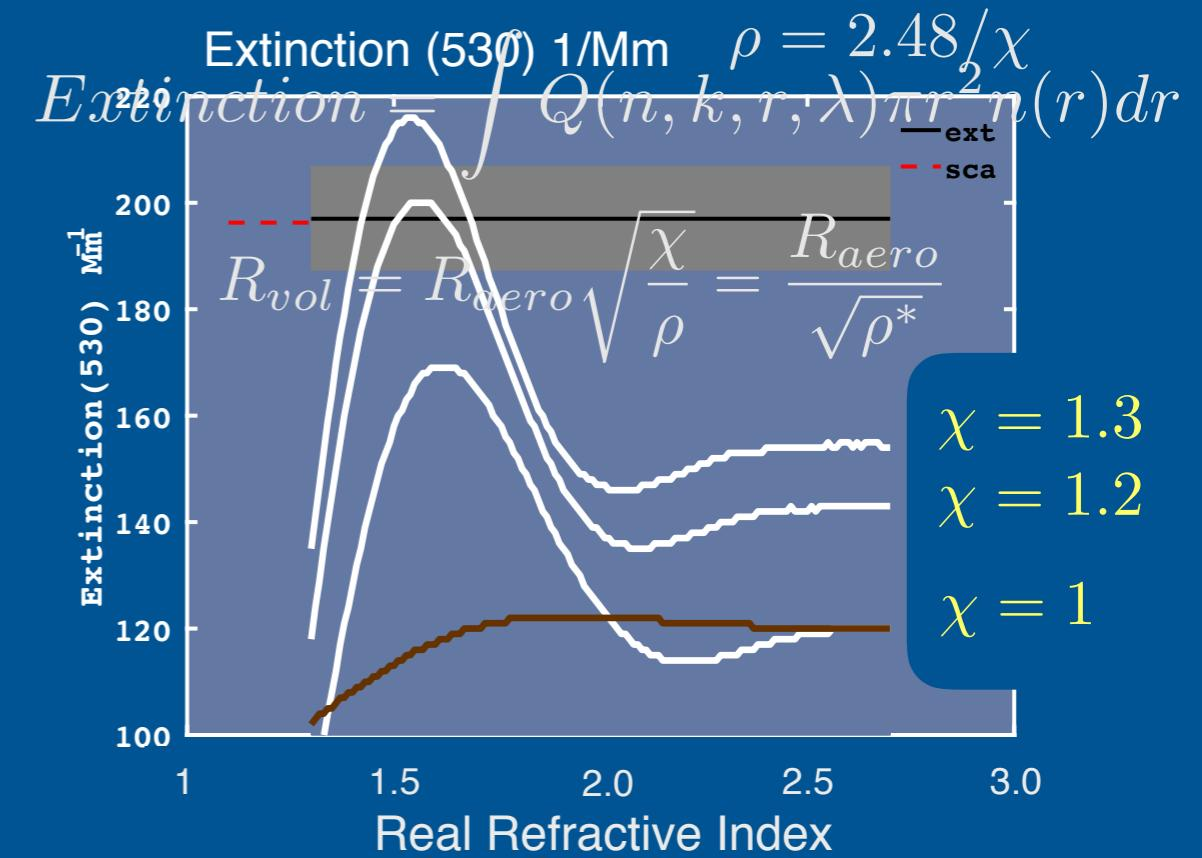
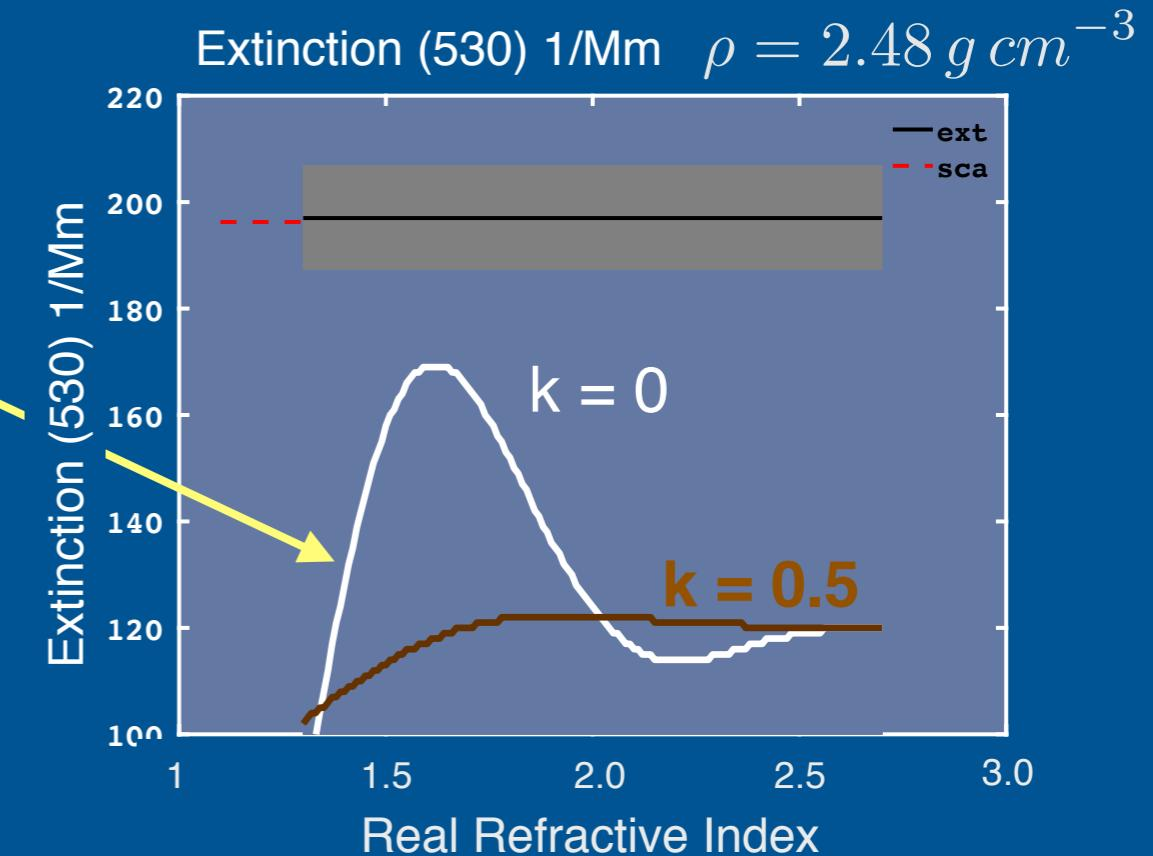
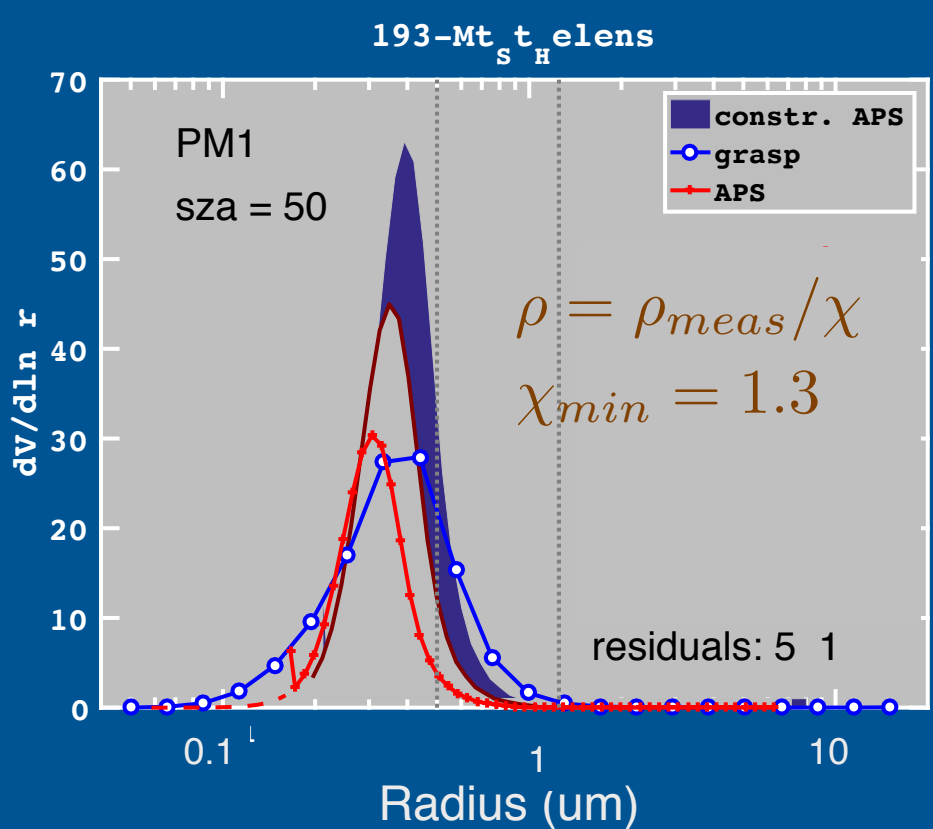
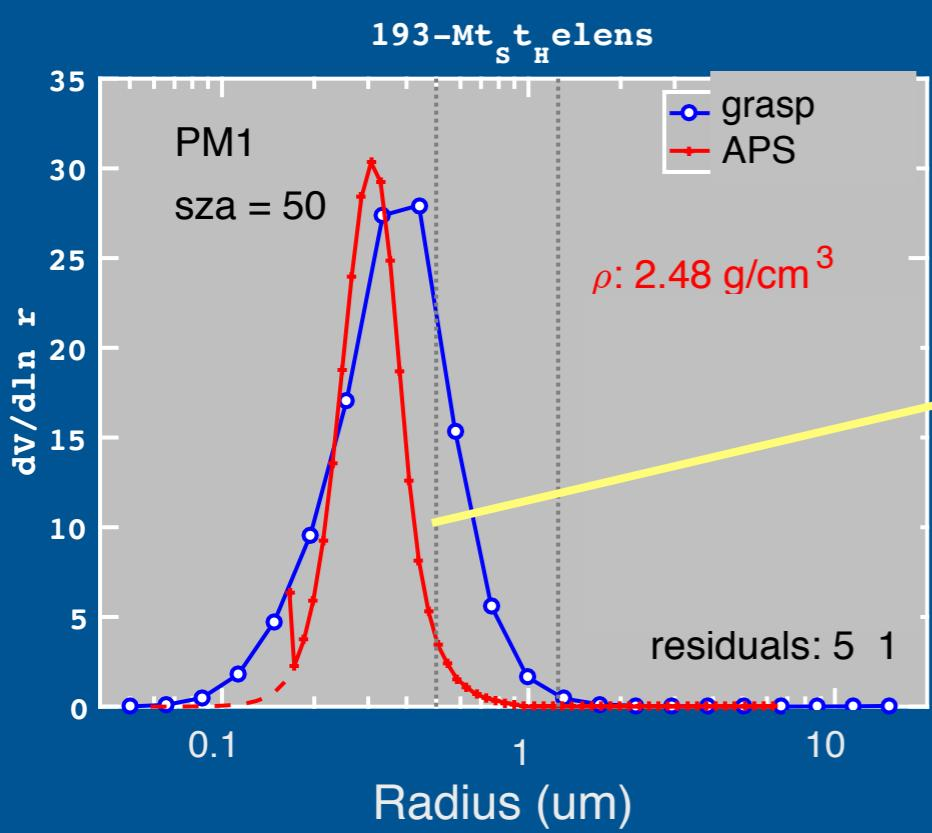
## GRASP residuals as a function of extinction



Bars indicate the percentage of retrievals that satisfy the 8% requirement in each extinction bin.

# Aerodynamic-Optical Size Conversion

Require closure with extinction measurements



# Comparing Retrieved Size Distributions to Aerodynamic Size

Evaluate size distribution retrievals using the effective variance and effective radius.

$$r_{eff} = \frac{\int r \times \pi r^2 n(r) dr}{\int \pi r^2 n(r) dr}$$

$$v_{eff} = \frac{\int (r - r_{eff})^2 \times \pi r^2 n(r) dr}{r_{eff}^2 \int \pi r^2 n(r) dr}$$

$$\chi = 1$$

$$\rho^* = \rho/\chi = \rho/1.3$$

